

# The Formation of a Helium White Dwarf in Close Binary System with Diffusion

O. G. Benvenuto<sup>1,2\*</sup> M. A. De Vito<sup>1†</sup>

<sup>1</sup> *Facultad de Ciencias Astronómicas y Geofísicas, Universidad Nacional de La Plata, Paseo del Bosque S/N, (1900) La Plata, Argentina*

<sup>2</sup> *Departamento de Astronomía y Astrofísica, Pontificia Universidad Católica, Vicuña Mackenna 4860, Casilla 306, Santiago, Chile*

December 30

## ABSTRACT

We study the evolution of a system composed by a  $1.4 M_{\odot}$  neutron star and a normal, solar composition star of  $2 M_{\odot}$  in orbit with a period of 1 day. Calculations were performed employing the binary hydro code presented in Benvenuto & De Vito (2003) that handle the mass transfer rate in a fully implicit way. Now we included the main standard physical ingredients together with diffusion processes and a proper outer boundary condition. We have assumed fully non - conservative mass transfer episodes.

In order to study the interplay of mass loss episodes and diffusion we considered evolutionary sequences with and without diffusion in which all Roche lobe overflows (RLOFs) produce mass transfer. Another two sequences in which thermonuclearly-driven RLOFs are not allowed to drive mass transfer have been computed with and without diffusion. To our notice, this study represents the first binary evolution calculations in which diffusion is considered.

The system produces a helium white dwarf of  $\sim 0.21 M_{\odot}$  in an orbit with a period of  $\sim 4.3$  days for the four cases. We find that mass transfer episodes induced by hydrogen thermonuclear flashes drive a tiny amount of mass transfer. As diffusion produces stronger flashes, the amount of hydrogen - rich matter transferred is slightly higher than in models without diffusion.

We find that diffusion is the main agent in determining the evolutionary timescale of low mass white dwarfs even in presence of mass transfer episodes.

**Key words:** stars: evolution - stars: interiors - stars: binary

## 1 INTRODUCTION

At present, it is a well established fact that low mass white dwarf (WD) stars should be formed during the evolution in close binary systems (CBSs). These objects are expected to have a helium rich interior simply because they have a mass below the threshold for helium ignition of about  $0.45 M_{\odot}$ . If they were formed as consequence of single star evolution, we would have to wait for timescales far in excess of the present age of the Universe to find some of them.

Formation of helium WDs in CBSs was first investigated long ago by Kippenhahn, Kohl & Weigert (1967) and Kippenhahn, Thomas & Weigert (1968). They found that

these objects are formed during the evolution of low mass CBSs and that the cooling evolution is suddenly stopped by thermonuclear flashes that are able to swell the star up to produce further Roche lobe overflows (RLOFs).

Since sometime ago, low mass WDs have been discovered as companions to millisecond pulsars (MSP). This fact sparked interest in helium WDs in order to investigate the deep physical links between both members of a given pair. In particular, it represents an attractive possibility to infer characteristics of the neutron star behaving as a MSP by studying the WD in detail. Studies devoted to helium WD properties are those of Alberts, et al. (1996); Althaus & Benvenuto (1997); Benvenuto & Althaus (1998); Hansen & Phinney (1998a); Driebe, et al. (1998); Driebe, et al. (1999); Schönberner, Driebe, & Blöcker (2000); Althaus & Benvenuto (2000); Althaus, Serenelli, & Benvenuto (2001abc); Serenelli, et al. (2001); Rohrmann, et al. (2002); Serenelli, et al. (2002). Sarna, Ergma, & Gerskevitš-Antipova (2000) considered the problem in the frame of detailed binary evolu-

\* Member of the Carrera del Investigador Científico, Comisión de Investigaciones Científicas de la Provincia de Buenos Aires (CIC), Argentina. Emails: obenvenuto@fcaglp.unlp.edu.ar; obenvenuto@astro.puc.cl

† Fellow of the CIC. Email: adevito@fcaglp.unlp.edu.ar

tion calculations. More recently, Podsiadlowski, Rappaport, & Pfahl (2002) have also computed the evolution of some CBS configurations that give rise to the formation of helium WDs. Also, Nelson & Rappaport (2003) have explored in detail the evolutionary scenarios of binary systems with initial periods shorter than the bifurcation one leading to the formation of ultra-compact binaries with periods shorter than an hour. On the opposite, in this paper we shall deal with a system with an initial period larger than the bifurcation one leading to wider binaries.

Remarkably, the first WD found as companion of a MSP in globular clusters has been detected by Edmonds et al. (2001). Among recent observations of low mass WD companion to MSPs we should quote those by van Kerkwijk et al. (2000) who have detected the WD companion of the binary MSP PSR B1855+09, whose mass is known accurately from measurements of the Shapiro delay of the pulsar signal,  $M_{WD} = 0.258^{+0.028}_{-0.016} M_{\odot}$ . The orbital period of this binary MSP is 12.3 days. More recently, Bassa, van Kerkwijk & Kulkarni (2003) have found a faint bluish counterpart for the binary MSP PSR J02018+4232. The spectra confirm that the companion is a helium WD and, in spite that observations are of insufficient quality to put a strong constraint on the surface gravity, the best fit indicates a low  $\log g$  value and hence low mass ( $\approx 0.2 M_{\odot}$ ). On the other hand, independently, Ferraro et al. (2003) and Bassa et al. (2003) have identified the optical binary companion to the MSP PSR J1911-5958A, located in the halo of the galactic globular cluster NGC 6752. This object turned out to be a blue star whose position in the color-magnitude diagram is consistent with the cooling sequence of a low-mass ( $\approx 0.17-0.20 M_{\odot}$ ), low metallicity helium WD at the cluster distance. This is the second helium WD with a mass in this range that has been found to orbit a MSP in a galactic globular cluster. Also, Sigurdsson, et al. (2003) have detected two companions for the pulsar B 1620-26, one of stellar mass and one of planetary mass. The color and magnitude of the stellar companion indicate a WD of  $0.34 \pm 0.04 M_{\odot}$  of age  $4.8 \times 10^8$  y. For previous detections of this kind of objects we refer the reader to the paper by Hansen & Phinney (1998b).

From a theoretical point of view, it was soon realized that the key ingredient of WD models is the hydrogen mass fraction in the star. Consequently, this called for a detailed treatment of the outer layers of the star. Iben & MacDonald (1985) demonstrated the relevance of diffusion in the evolution of intermediate mass CO WDs while Iben & Tutukov (1986) found it to be also important in low mass WDs.

More recently, Althaus, et al. (2001abc) revisited the problem of the formation of helium WDs. In doing so, they mimicked binary evolution by abstracting mass to a  $1 M_{\odot}$  object on the RGB. The main goal of these papers was to investigate in detail the role of diffusion during the evolution as a pre-WD object. They allowed gravitational settling, chemical and thermal diffusion to operate. However, they did not consider the possibility of any mass transfer episode after detachment from the RGB. Perhaps the main result of Althaus, et al. (2001abc) was the finding that for models with diffusion there exists a threshold mass value  $M_{th}$  above which the object undergoes several thermonuclear flashes in which a large fraction of the hydrogen present in the star is burnt out. Consequently, as the star enters on the final cooling track it evolves fast, reaching very

low luminosities on a timescale comparable with the age of the Universe. Quite contrarily, in models without diffusion, evolutionary timescales are much longer, making it difficult to reconcile with observations. For WDs belonging to CBSs in companion with MSP, WD ages should be comparable to the characteristic age of pulsars  $\tau_{PSR} = P/2\dot{P}$  (for a pulsar of period  $P$  with period derivative  $\dot{P}$  that had an initial period  $P_0$  such that  $P_0 \ll P$  and braking index  $n = 3$ ). This should be so, because it is generally accepted that the MSP is recycled by accretion from its normal companion. However, it was found that the WD was much dimmer than predicted by models without diffusion, which should be interpreted as consequence of a faster evolution. This has been the case of the companion of PSR B1855+09.

For objects with masses below  $M_{th}$  no thermonuclear flash occurs and the star does not suffer from another RLOF. Consequently, it retains a thick hydrogen layer, able to support nuclear burning, forcing the WD to remain bright for a very long time. This is the case of the companion of PSR J1012+5307.

It is the aim of the present paper to revisit the problem of the formation and evolution of helium WDs in CBSs by performing full binary computations considering diffusion starting with models on the main sequence all the way down to stages of evolution of the remnant as a very cool WD. To our notice this is the first time such a study is carried out. In this way we largely generalize the previous studies from our group on this topic. In doing so, we have preferred to concentrate on a particular binary system, deferring a detailed exploration of the huge parameter space (masses, orbital periods, chemical compositions, etc.) to future publications. To be specific, we have chosen to study a CBS composed by a  $2 M_{\odot}$  normal star together with a neutron star with a ‘‘canonical’’ mass of  $1.4 M_{\odot}$  on an initial orbit of 1 day of period. We assumed solar chemical composition with  $Z = 0.02$  for which  $M_{th} \approx 0.19 M_{\odot}$  (Althaus et al. 2001b).

In order to explore the role and interplay of mass loss episodes and diffusion we have constructed four complete evolutionary calculations:

- Case A: Diffusion, all RLOF operate (including flash-induced RLOF)
- Case B: Diffusion, without flash-induced RLOF
- Case C: No diffusion, all RLOF operate
- Case D: No diffusion, without flash-induced RLOF

Regarding mass transfer episodes we have chosen to study the case of fully non conservative conditions, i.e., those in which all the matter transferred from the primary star is lost from the system carrying away all its intrinsic angular momentum. We do so in order to get the strongest possible RLOFs which, in turn, will produce the largest mass transfer episodes. In this sense, we shall get an upper limit to the effects of RLOFs on the whole evolution of the star, in particular regarding the ages of very cool WDs.

The remainder of the paper is organized as follows. In Section 2 we describe our code paying special attention to the changes we implemented in the scheme for computing mass transfer episodes. Then, in Section 3 we describe the evolutionary results for the four cases considered here. Finally, in 4 we discuss the implications of our calculations and summarize the main conclusions of this work.

## 2 NUMERICAL METHODS

In the computations presented below we have employed the code for computing stellar evolution in close binary systems presented in Benvenuto & De Vito (2003). Now we have incorporated the full physical ingredients with the aim of getting state-of-the-art evolutionary results. In particular, we have included a complete set of nuclear reactions to describe hydrogen and helium burning together with diffusion processes. For more details on the considered physics, see, e.g., Althaus, et al. (2001a).

Regarding the outer boundary condition, we have incorporated the formula given by Ritter (1988) for computing the mass transfer rate  $\dot{M}$ :

$$\dot{M} = -\dot{M}_0 \exp\left(-\frac{R_L - R}{H_P}\right); \quad (1)$$

where  $\dot{M}_0$  is the MTR for a star that exactly fills the Roche lobe (see Ritter's paper for its definition),  $R_L$  is the equivalent radius of the Roche lobe (see below),  $R$  is the stellar radius and  $H_P$  is the photospheric pressure scale height. We have considered that a mass transfer episode is underway when  $R \geq R_L - \xi H_P$  with  $\xi = 16$ . In this way the star begins (ends) to transfer mass in a very natural and smooth way. This has been completely adequate for the purpose of carrying out the calculations presented below.

## 3 EVOLUTIONARY CALCULATIONS

In order to present the numerical calculations we shall describe in detail the sequence for which all physical ingredients were considered (Case A) in which we allowed diffusion and mass transfer in each RLOF to operate. The evolutionary track in the HR diagram corresponding to case A is shown in Fig. 1. The  $2 M_\odot$  object begins to evolve and the first RLOF occurs (point 1 in Table 1) when it is still burning hydrogen in the center. Thus, we are dealing with Class A mass transfer, as defined by Kippenhahn & Weigert (1967). At that moment the hydrogen central abundance is  $X_H = 0.214578$ . From there on, as consequence of the orbital evolution of the binary, the primary star undergoes a huge mass loss (see the first panel of Fig. 2) which continues up to the moment (point 2 in Table 1) at which central hydrogen exhaustion occurs. The star contracts and mass transfer is stopped; at that moment the mass of the primary is of  $1.59252 M_\odot$ . Little later, as consequence of the formation of a shell hydrogen burning zone, the star inflates and mass transfer starts again (point 3), and stands on a long period at which the star loses almost 90% of the initial mass, ending with a mass of  $0.22007 M_\odot$ . Hereafter we shall consider these *two* RLOF episodes as an *initial* RLOF in order to differentiate it from the other flash-induced RLOFs. During the initial mass transfer episode, the hydrogen content of the outermost layers dropped up to a minimum value of  $\approx 0.3$  because mass transfer dredges up layers that were previously undergoing appreciable nuclear burning (see Fig. 3). This increase in the mean molecular weight of the plasma present in the outer layers of the star favours the contraction of the primary star. At point 4 the star detaches from the Roche lobe, and since then on the star evolves bluewards very fast up to approximately the moment at which reaches a local

maximum in the effective temperature. After such maximum effective temperature, evolution appreciably slows down allowing diffusion to have time enough to sensibly evolve the hydrogen profile. Here, hydrogen tends to float simply because it is the lighter element present in the plasma. This is clearly shown as a steep increase in Fig. 3 where we show the surface hydrogen abundance<sup>1</sup> of the model as a function of time.

Quite in contrast with the behaviour of surface abundance, at the bottom of the hydrogen envelope, hydrogen tend to sink now as a consequence of large abundance gradients. The net effect is that, while the outer layers get richer in hydrogen, diffusion is fueling hot layers. Then, when the hydrogen rich layers become degenerate and conduction eases the energy flux outwards, hydrogen becomes hot enough to ignite. Now, in degenerate conditions, ignition is unstable (See Fig. 4). Consequently, evolution suddenly accelerates and there occurs a hydrogen thermonuclear flash. Such a flash is not strong enough to inflate the star to force a new RLOF. Regarding surface abundances, we should remark that little time after thermonuclear flash occurs, the star develops a deep outer convective zone embracing from very hydrogen rich layers up to others in which hydrogen is almost a trace. As consequence, hydrogen abundance suddenly drops<sup>2</sup> down to a value similar to the one the star had at the end of the initial RLOF (see Fig. 3 and Table 1). The referred mixing is noticeable in the evolutionary track (Fig. 1) as a sudden change of slope after the minimum in the effective temperature and luminosity of the star. After mixing, the outer layers of the star continue swelling up to get near producing a RLOF, but begin to contract before. After maximum radius is reached, the star undergoes a fast contraction up to its maximum effective temperature, and thereon again timescales become long enough for diffusion to operate. The star again floats hydrogen at outer layers and fuel others that will make the star to undergo a second thermonuclear flash. Now the star has a higher degree of degeneracy in the critical layers, making the flash to be stronger than the previous one. From there on the star undergoes much the same evolution as in the previous flash, but now the star inflates enough to undergo a third RLOF event. The conditions at the onset of this third RLOF correspond to point 5 in Table 1.

Obviously, this third RLOF is deeply different to the initial one. Now the envelope is very dilute and so, a tiny amount of stellar mass occupy a large portion of its radius. Consequently, very little mass is transferred from the primary in contrast with initial RLOF in which the primary transferred about 90% of its initial mass. The MTR during this third RLOF is depicted in the third panel of Fig. 2. Remarkably, the mass lost from the primary star during this third RLOF has a low hydrogen abundance due to the previous mixing.

After few thousands of years transferring mass, the star contracts again repeating essentially the same evolution the star followed after the first thermonuclear flash. However, re-

<sup>1</sup> As a matter of facts this is the abundance of the first point of the discrete mesh of the model, located at  $\log 1 - M_r/M \approx -8$ .

<sup>2</sup> Notice that this is consequence of the fact that we have assumed instantaneous mixing throughout convective zones.

**Table 1.** Selected stages of the evolution of a system composed by a  $1.4 M_{\odot}$  neutron star and a normal, solar composition star of  $2 M_{\odot}$  in orbit with an initial period of 1 day. Here we have considered diffusion and mass transfer during each RLOF episode (Case A). Points labeled with odd (even) numbers correspond to the beginning (end) of a mass transfer episode in Fig. 1. The last point corresponds to the end of the computation.

Point	$\log(L/L_{\odot})$	$\log(L_{nuc}/L_{\odot})$	$\log(T_{eff})$	$X_s$	Age [Myr]	$M_*/M_{\odot}$	$P$ [d]	$M_H/M_*$
0	1.291596	1.291596	3.999353	0.700000	0.000000	2.00000	1.000	0.700000
1	1.306425	1.325886	3.883615	0.719213	675.907133	2.00000	0.990	0.631826
2	1.069236	1.085928	3.808278	0.700722	898.696085	1.59252	1.273	0.593744
3	1.052254	1.083202	3.803819	0.700938	899.305975	1.59252	1.273	0.593691
4	1.007000	0.998083	3.774765	0.297839	1057.346100	0.22007	4.309	0.029015
5	2.158183	1.557922	4.071799	0.213738	1126.419320	0.22007	4.309	0.005668
6	2.310374	1.558437	4.115358	0.213738	1126.419557	0.21990	4.310	0.005490
7	2.151000	1.900315	4.068010	0.172838	1149.826078	0.21990	4.310	0.004322
8	2.521391	1.900161	4.170841	0.172838	1149.826261	0.21919	4.313	0.003738
9	2.210319	2.297033	4.080971	0.119486	1214.483908	0.21919	4.313	0.002783
10	2.754083	2.360036	4.233749	0.119486	1214.484019	0.21801	4.320	0.002141
11	-5.001480	$-\infty$	3.352189	0.998488	18995.499104	0.21801	4.316	0.001609

markably, the star has lost hydrogen, due to nuclear burning as well as to mass transfer (see Fig. 5). However, the star still has an amount of hydrogen high enough to force the star to undergo another flash. Now the flash is rather more violent than the previous one producing another RLOF.

In order to gain clarity, we have chosen to discuss in detail the loop due to the last thermonuclear flash. In Fig. 6 we show the excursion of the star in the HR diagram indicating the main physical agents acting in the star together with some particular models (solid dots). The hydrogen profiles corresponding to models before and just at the end of (after) the RLOF are shown in Fig. 7 (Fig. 8). Some relevant characteristics of these models are presented in Table 2.

The hydrogen profile for some of the models indicated in Fig. 7 corresponding to stages previous to and just after the last RLOF. Up to model labeled 11000 (the model number in the sequence) the outwards motion of the profile is due to the nuclear burning during the flash. Since model 11000 (not shown in the figure) the profile moves outwards as consequence of the mass transfer episode which ends in the model 11200. Notice that the loss of hydrogen is somewhat tiny (points 9 and 10 in Table 1).

In Fig. 8 curve labeled as 14500 corresponds to stages somewhat after RLOF. Curves labeled as 15000 - 15050 are displaced outwards due to nuclear burning while curve 15075 corresponds to a profile modified by diffusion. Notice the tail of the hydrogen profile gets appreciably deeper approximately when the outermost layers become saturated by hydrogen.

From our calculations we find that only after *four* hydrogen thermonuclear flashes the star is able to enter on the final cooling track of a helium WD (see Fig. 4). The evolutionary timescale of the model is presented in Fig. 9. Notice that the nuclear energy release at such advanced stages of evolution is a minor contribution to the total energy balance of the star. As consequence the star gets heat from its relic thermal content which forces a fast evolution, reaching very low luminosities in timescales comparable to the age of the Universe. We stopped the calculation when the object reached  $\log L/L_{\odot} = -5$ , at that moment the star had an age of about 19 Gyr.

Now, let us discuss the results corresponding to Case

C in which we allowed all RLOF to drive mass transfer but we have neglected diffusion (see Table 3). The evolutionary track for this case is shown in Fig. 1, panel C. Here, the evolution previous to the end of the initial RLOF is very similar to that corresponding to the Case A. In other words, diffusion has a negligible effect on these evolutionary stages. Perhaps, the main difference is the increase in hydrogen surface abundances previous to the initial RLOF found in Case A is absent here (see Table 1). However, differences in the evolution are quite significantly after the end of initial RLOF.

As here, by assumption, the physical agents able to modify abundances are only nuclear reactions and convection, obviously, the outermost layers of the hydrogen - rich layers are not enriched by hydrogen and simultaneously no fueling occurs at the bottom. Consequently, the evolution is very different. Notably, the star undergoes only three thermonuclear flashes and outer layers have rather constant abundances in spite that they also develop outer convection zones after each flash. As in the previous case we computed the evolution up to when the object reached  $\log L/L_{\odot} = -5$  with an age of about 25.65 Gyr. Thus, evolution is markedly slower than in Case A. This is due to the fact that here thermonuclear flashes are weaker, burning less hydrogen. As consequence, the star is able to undergo appreciable thermonuclear energy release during the final cooling track as a helium WD. In this regard, notice that nuclear burning remains the dominant energy source of the star up to ages of 10 Gyr (see Fig. 9).

The sequence of models corresponding to Case B (Case C) is very similar to that corresponding to Case A (Case D) and will not be discussed in detail. The obvious major difference is related to the size the star is able to reach just after thermonuclear flashes. As in Case B (case D) it is assumed that there is no limitation imposed by the size of the Roche lobe, after thermonuclear flashes, the star reaches effective temperatures far lower than those allowed in the case of the occurrence of RLOFs. Quite noticeably, the evolutionary timescale of the final WD cooling track is largely independent of the occurrence of any thermonuclear flash - induced RLOF (see Fig. 9).

Another interesting difference arises regarding the char-

**Table 2.** Selected stages of the evolution of the primary star of the system corresponding to Case A. We have selected relevant models in a loop shown at Fig. 6. Model stand for the number of models in the evolutionary calculation.

Model	$\text{Log}(L/L_\odot)$	$\text{Log}(L_{nuc}/L_\odot)$	$\text{Log}(T_{eff})$	$X_s$	Age [Myr]	$M_H/M_*$
9561	-1.285417	-1.464898	4.136383	0.997875	1206.136861	0.002962
9593	-0.743989	1.319834	4.227583	0.997875	1214.482831	0.002921
9607	-0.859529	2.616561	4.191011	0.997875	1214.483706	0.002915
9719	-1.700589	4.860120	3.878964	0.997875	1214.483802	0.002820
9840	-1.577785	4.118219	3.784233	0.997875	1214.483809	0.002790
10482	0.378350	2.338424	3.877158	0.119486	1214.483895	0.002783
10642	2.014473	2.313509	4.127957	0.119486	1214.483902	0.002783
10714	2.210319	2.297033	4.080971	0.119486	1214.483908	0.002783
11190	2.754083	2.360036	4.233749	0.119486	1214.484019	0.002141
12187	2.390152	2.739479	4.464822	0.119486	1214.484802	0.002120
14693	1.948789	1.939478	4.613450	0.120118	1214.493795	0.002062
15039	-0.774868	-1.657584	4.278570	0.395631	1215.485203	0.001664
15050	-1.112451	-2.015089	4.205475	0.720579	1216.420781	0.001664
15055	-1.281705	-2.151893	4.167198	0.921884	1217.429788	0.001663
15075	-1.805696	-2.445395	4.045660	0.998488	1267.968504	0.001653

**Table 3.** Selected stages of the evolution of a system composed by a  $1.4 M_\odot$  neutron star and a normal, solar composition star of  $2 M_\odot$  in orbit with a period of 1 day. Here mass transfer is allowed to occur during each RLOF episode but diffusion has been neglected (Case C). Points labeled with odd (even) numbers correspond to the beginning (end) of a mass transfer episode. The last point corresponds to the end of the computation.

Model	$\text{Log}(L/L_\odot)$	$\text{Log}(L_{nuc}/L_\odot)$	$\text{Log}(T_{eff})$	$X_s$	Age [Myr]	$M_*/M_\odot$	$P$ [d]	$M_H/M_*$
0	1.291596	1.291596	3.999353	0.700000	0.000000	2.00000	1.000	0.700000
1	1.305931	1.325651	3.883688	0.700000	683.258119	2.00000	0.990	0.631100
2	1.080234	1.081842	3.811255	0.699873	892.518745	1.60119	1.266	0.595018
3	1.059051	1.092015	3.805732	0.699873	893.302911	1.60119	1.266	0.594950
4	1.011273	0.998631	3.776142	0.297567	1049.362320	0.22033	4.307	0.028800
5	2.147837	1.441249	4.068767	0.224255	1116.384319	0.22033	4.307	0.005821
6	2.297723	1.446788	4.111879	0.224255	1116.384550	0.22018	4.308	0.005645
7	2.099698	1.812834	4.054606	0.196021	1153.232534	0.22018	4.308	0.004501
8	2.520010	1.808553	4.171450	0.196021	1153.232711	0.21943	4.312	0.003816
9	-5.011041	$-\infty$	3.356698	0.196019	25653.632359	0.21943	4.308	0.001758

acteristic timescale of evolution of the models from the red part of the diagram to the maximum effective temperature conditions. We have found that in such stages, evolution of models for which thermonuclearly induced RLOFs are allowed suffer from a much faster evolution regardless of the allowance or not of diffusion. To be specific, from minimum to maximum effective temperature, Case B models take  $\approx 10^6$  y while models with RLOF spend only  $\approx 10^4$  y from Roche lobe detachment to maximum effective temperature. This, obviously indicates that it should be more difficult to find objects at such conditions than predicted in models without thermonuclearly - induced RLOFs. Also, notice in Fig. 1 that the subflashes (little loops in the evolutionary tracks occurring when the star is evolving bluewards) happen at different effective temperatures depending on the allowance of RLOFs. In fact, in models with (without) RLOFs subflashes occur at higher (lower) effective temperatures for consecutive thermonuclear flashes. This is so irrespective of allowance or not of diffusion.

## 4 DISCUSSION AND CONCLUSIONS

In this work we have computed the evolution of a binary system composed by a neutron star with a ‘‘canonical mass’’ of  $1.4 M_\odot$  and a normal, population I main sequence star of  $2 M_\odot$  in orbit with a 1 day period. We have performed the calculations employing an updated version of the code presented in Benvenuto & De Vito (2003) in which we have included the main standard physical ingredients together with diffusion processes. Also a proper outer boundary condition was incorporated following Ritter (1988) (see §2).

In order to explore the role of mass transfer episodes from the primary star and its interplay with diffusion we have considered four situations: diffusion, all RLOF operate (Case A); diffusion, no flash - induced RLOF operates (Case B); no diffusion, all RLOF operate (Case C); and no diffusion, no flash - induced RLOF operates (Case D). See introduction (§ 1) of further details.

To our notice, these calculations represent the first detailed study of binary evolution considering diffusion. In this sense, this work represents a natural generalization of the results presented by Althaus, Serenelli & Benvenuto (2001a) in which binary evolution processes was mimicked by forcing a  $1 M_\odot$  star on the red giant branch to undergo an appro-

priate mass loss rate. Now the proper inclusion of the specific processes that govern binary evolution offer us a more physically sound description of the formation of low mass, helium white dwarfs (WDs). In particular, now we have the possibility of connecting stellar structure and evolution with the orbital parameters of the systems allowing for a deeper comparison with observations.

From the results presented in the previous sections, it is clear that diffusion is far more important in determining the timescale of evolution of the stars than mass transfer episodes during flash - induced RLOFs. This is so especially when the object reaches the final cooling track. We found that timescales are almost insensitive to the occurrence of flash - induced RLOF episodes (see Fig. 9). This constitutes the main result of the present work.

## 5 ACKNOWLEDGMENTS

We thank our referee, Prof. Philipp Podsiadlowski for comments and suggestions that allowed to improve the clarity of the original version. OGB is supported by FONDAP Center for Astrophysics 15010003.

## REFERENCES

- Alberts, F., Savonije, G. J. van den Heuvel, E. P. J. & Pols, O. R. 1996, *Nature* 380, 676
- Althaus, L. G. & Benvenuto, O. G. 1997, *ApJ*, 477, 313
- Althaus, L. G. & Benvenuto, O. G. 2000, *MNRAS*, 317, 952
- Althaus, L. G., Serenelli, A. M., & Benvenuto, O. G. 2001a, *ApJ*, 554, 1110
- Althaus, L. G., Serenelli, A. M., & Benvenuto, O. G. 2001b, *MNRAS*, 324, 617
- Althaus, L. G., Serenelli, A. M., & Benvenuto, O. G. 2001c, *MNRAS*, 323, 471
- Bassa, C. G., van Kerkwijk, M. H., & Kulkarni, S. R. 2003, *A&A*, 403, 1067
- Bassa, C. G., Verbunt, F., van Kerkwijk, M. H., & Homer, L. 2003, *A&A*, 409, L31
- Benvenuto, O. G. & Althaus, L. G. 1998, *MNRAS*, 293, 177
- Benvenuto, O. G. & De Vito, M. A. 2003, *MNRAS*, 342, 50
- Driebe, T., Schoenberner, D., Bloeker, T., & Herwig, F. 1998, *A&A*, 339, 123
- Driebe, T., Blöcker, T., Schönberner, D., & Herwig, F. 1999, *A&A*, 350, 89
- Edmonds, P. D., Gilliland, R. L., Heinke, C. O., Grindlay, J. E., & Camilo, F. 2001, *ApJ*, 557, L57
- Ferraro, F., Possenti, A., Sabbi, E., & D'Amico, N. 2003, *ApJ*, 596, L211
- Hansen, B. M. S. & Phinney, E. S. 1998a, *MNRAS*, 294, 557
- Hansen, B. M. S. & Phinney, E. S. 1998b, *MNRAS*, 294, 569
- Iben, I. & MacDonald, J. 1985, *ApJ*, 296, 540
- Iben, I. J. & Tutukov, A. V. 1986, *ApJ*, 311, 742
- Kippenhahn, R., Kohl, K., Weigert, A. 1967, *Zap*, 66, 58
- Kippenhahn, R., Thomas, H.-C., Weigert, A. 1968, *Zap*, 69, 265
- Kippenhahn, R., Weigert, A. 1967, *Zap*, 65, 251
- Nelson, L. A. & Rappaport, S. 2003, *ApJ*, 598, 431
- Podsiadlowski, P., Rappaport, S., & Pfahl, E. D. 2002, *ApJ*, 565, 1107
- Ritter, H. 1988, *A&A*, 202, 93
- Rohrmann, R. D., Serenelli, A. M., Althaus, L. G., & Benvenuto, O. G. 2002, *MNRAS*, 335, 499
- Sarna, M. J., Ergma, E., & Gerškevičš-Antipova, J. 2000, *MNRAS*, 316, 84
- Schönberner, D., Driebe, T., & Blöcker, T. 2000, *A&A*, 356, 929
- Serenelli, A. M., Althaus, L. G., Rohrmann, R. D., & Benvenuto, O. G. 2001, *MNRAS*, 325, 607
- Serenelli, A. M., Althaus, L. G., Rohrmann, R. D., & Benvenuto, O. G. 2002, *MNRAS*, 337, 1091
- Sigurdsson, S., Richer, H. B., Hansen, B. M., Stairs, I. H., & Thorsett, S. E. 2003, *Science*, 301, 193
- van Kerkwijk, M. H., Bell, J. F., Kaspi, V. M., & Kulkarni, S. R. 2000 *ApJ*, 530, L37

This paper has been typeset from a  $\text{\TeX}/\text{\LaTeX}$  file prepared by the author.

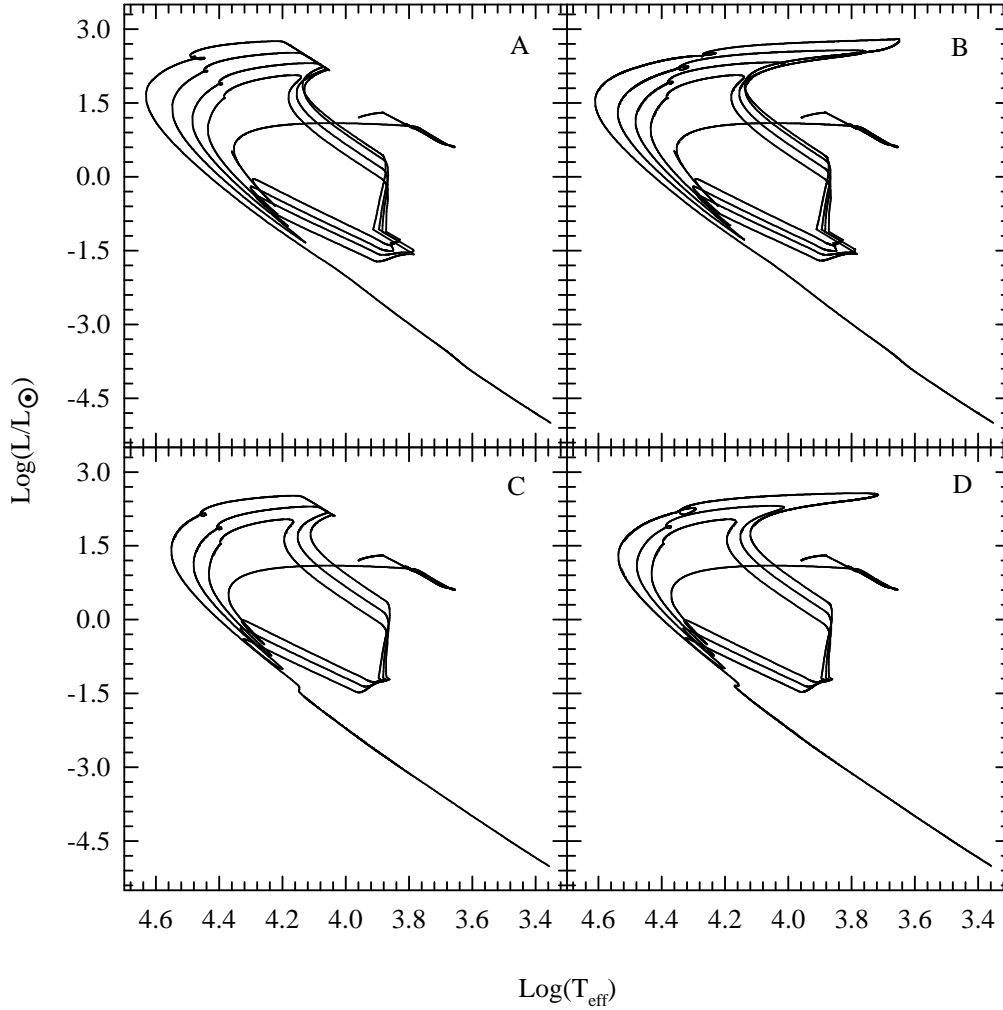


**Figure 1.** The evolutionary tracks for the primary component of the binary system initially composed by a normal main sequence, solar composition star of  $M = 2.0 M_{\odot}$  together with a neutron star of  $1.4 M_{\odot}$ , with a period of  $P = 1.0$  day for the four cases considered in this paper. Each panel is labeled as in the main text: **A:** diffusion, all RLOFs operate; **B:** diffusion, no flash - induced RLOF operates; **C:** no diffusion, all RLOFs operate; **D:** no diffusion, no flash - induced RLOF operates. Notice that models with diffusion suffer from four hydrogen thermonuclear flashes, while models without diffusion undergo only three. This is independent of considering or ignoring the flash - induced mass transfer episodes. Here, for the sake of clarity we decided not to indicate the points given in Tables 1 - 3

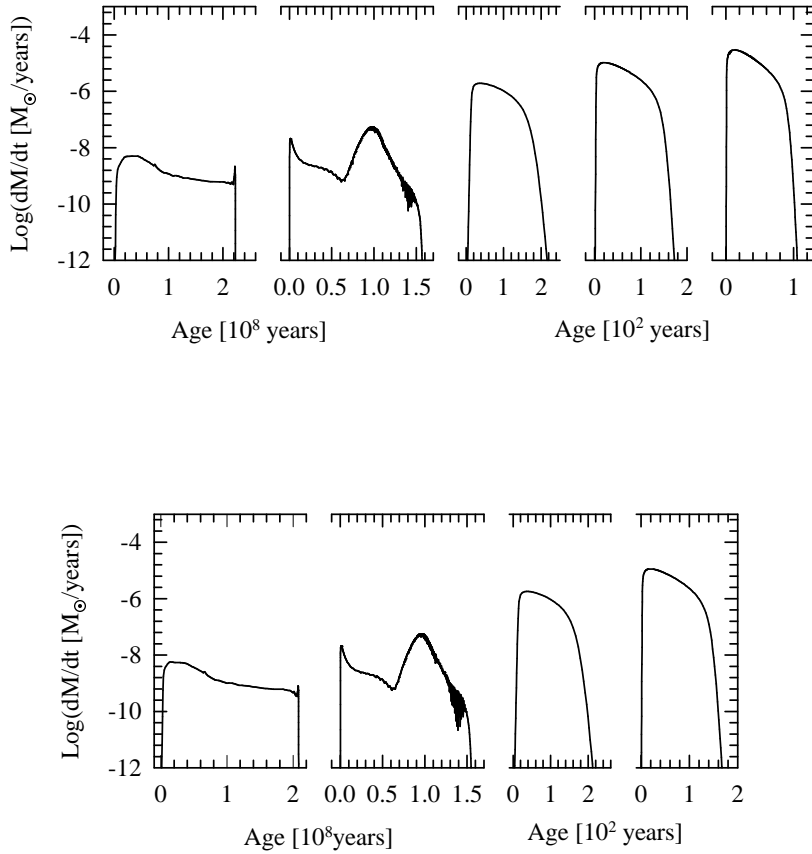


**Figure 2.** The mass transfer rates from the primary star corresponding to the evolutionary tracks shown in Fig. 1 in which mass transfer is considered at each RLOF. Upper panel corresponds to case **A** (with diffusion) while lower panel depicts the results for case **C** (without diffusion). From left to right panels correspond to each RLOF episode. For clarity, in each panel we have counted time since the beginning of each mass transfer episode. For the absolute value of time we simply have to add the time of the onset of RLOF given in Tables 1 and 3 respectively. Notice that, in both cases, the initial RLOF is very prolonged. The first happens when the star is still burning hydrogen at its core. At core exhaustion mass transfer ends, and when the star swells due to the outwards motion of the hydrogen shell burning, there occurs a new RLOF. We called these two RLOFs as the *initial* RLOF. In lower and upper panels these events are almost the same due to the fact that the effects of diffusion are barely noticeable at these early stages. The subsequent episodes are due to thermonuclear flashes. Notice that their duration is six orders of magnitude shorter.



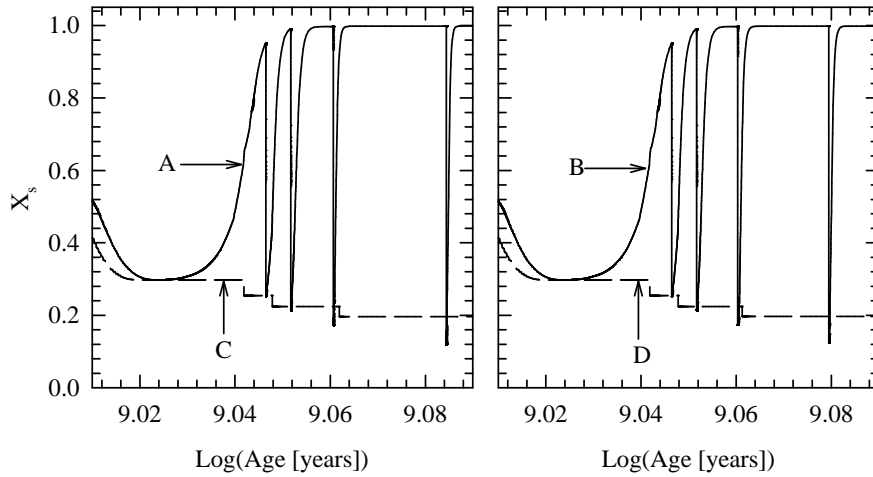


**Figure 3.** The hydrogen abundance in the outermost layers of the primary star. Here we considered the hydrogen abundance at the first point in the grid corresponding to  $1 - M_r/M \approx 10^{-8}$ . In the left panel we depict the results for models in which RLOFs are allowed whereas right panel depicts the case for models in which mass transfer driven by thermonuclearly induced RLOFs is neglected. Each curve is labeled as in Fig. 1. Notice the enormous differences in the behaviour of outer layers in the cases with and without diffusion. However, abundances are barely affected by allowance of mass transfer, as it is clearly noticeable in view of the similarities of the plots in each panel. In the sequences corresponding to case A, due to mixing, mass transferred during each RLOF has a chemical composition corresponding to a minimum in hydrogen abundance. Such a composition is very similar to that of the plasma transferred in the models of Case C without diffusion. See main text for further details.

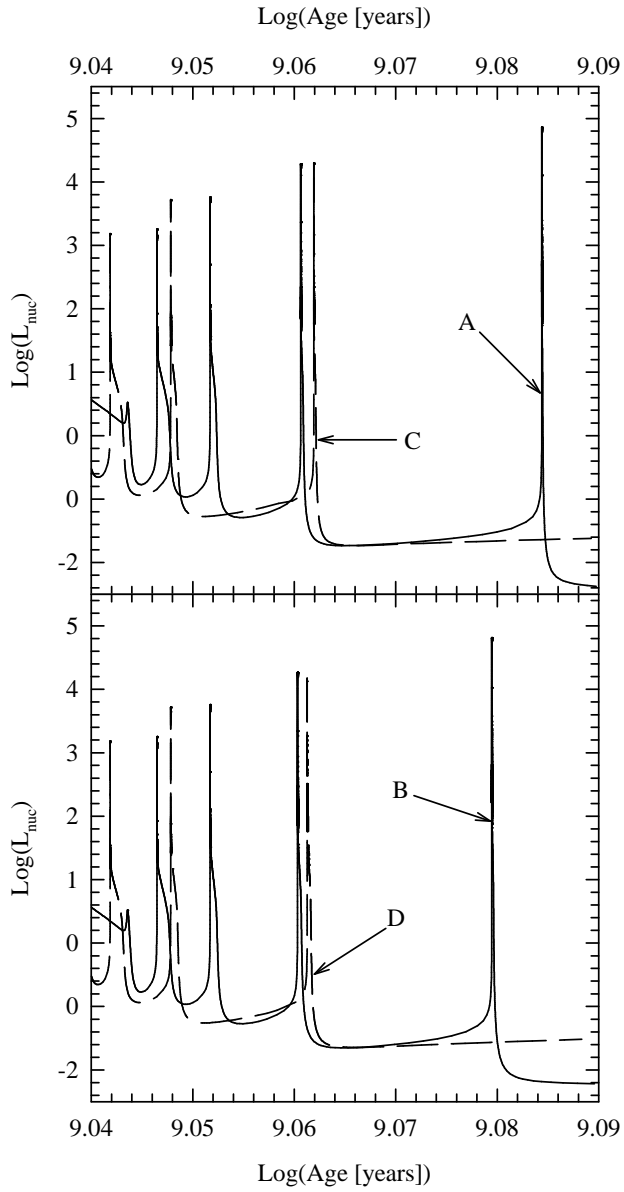


**Figure 4.** The logarithm of the nuclear luminosity (in solar units) vs. age relationship for the four evolutionary sequences studied in this paper. Labels A, B, C, D refer to the evolutionary tracks A to D in Fig. 1. Notice that models with (without) diffusion undergo four (three) thermonuclear flashes.

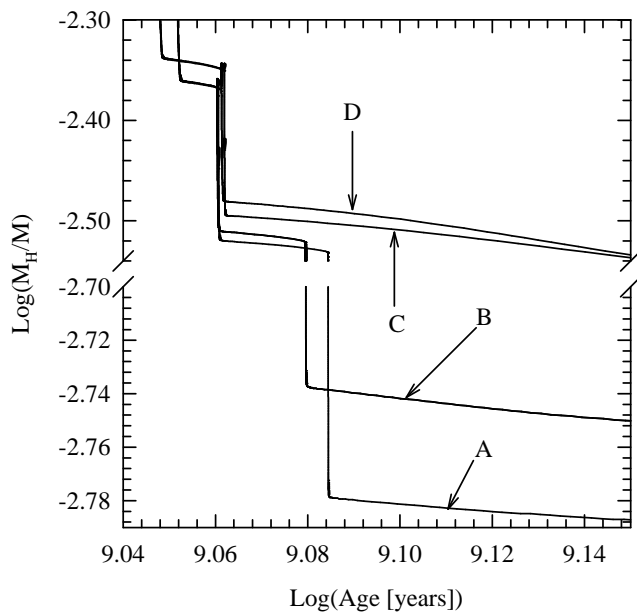


**Figure 5.** The logarithm of the hydrogen mass fraction present in the star vs. time for the four cases of evolution presented in this paper during the last thermonuclear flashes. Labels A, B, C, D refer to the evolutionary tracks A to D in Fig. 1. Notice that after thermonuclear flashes, models with diffusion have a lower hydrogen fraction. Also, as it may be expected, the hydrogen mass fraction is lower for models in which RLOFs operate at these stages. Models without diffusion end their flash episodes with a higher hydrogen content which is subsequently burnt out during the final cooling track. Notice the change in the vertical scale of this figure above and below the break in the vertical axis. See main text for further details.

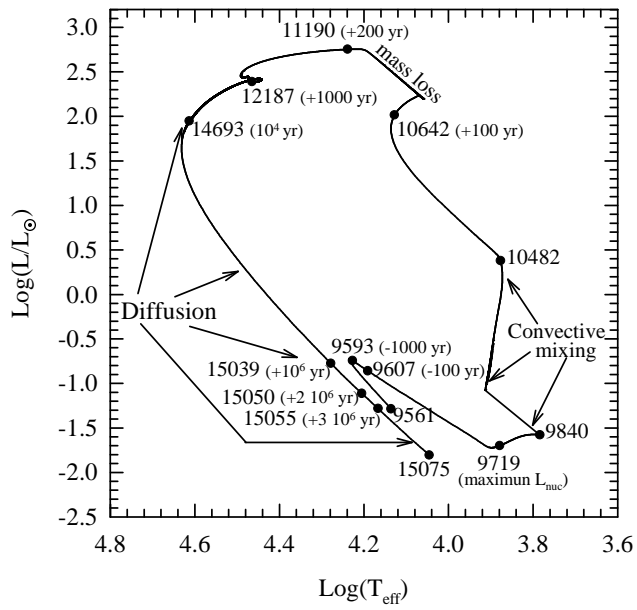


**Figure 6.** The last loop in the HR diagram corresponding to case A evolution. Solid dots correspond to selected stages, for some of which the hydrogen profiles are presented below and are labeled with the number of model in the computed sequence. Ages are counted with respect to the maximum in the nuclear energy release. We also remark the most important physical effects in each portion of the track. Notice the sudden changes in the shape of the track due to convective mixing and mass loss.

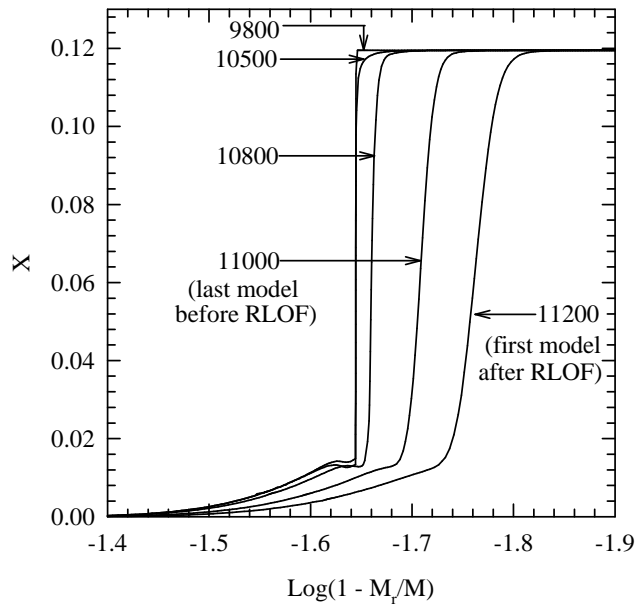


**Figure 7.** The hydrogen profile for some of the models indicated in Fig. 6 corresponding to stages previous to and just after the last RLOF. Up to model labeled 11000 the outwards motion of the profile is due to nuclear burning. From this model to the one labeled 11200 the motion is almost entirely due to the mass transfer during the RLOF.

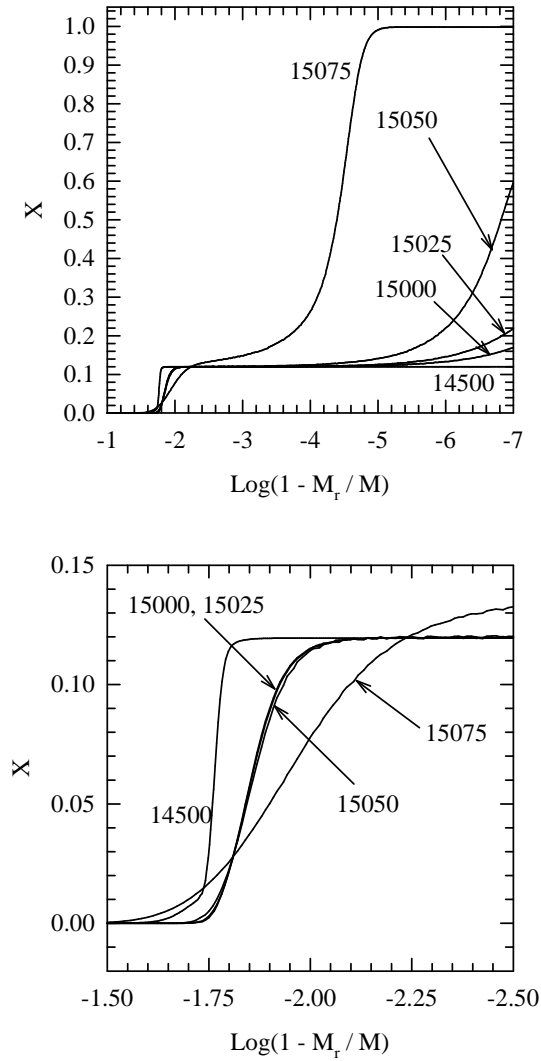


**Figure 8.** The hydrogen profile for some of the models indicated in Fig. 6 corresponding to stages after the last RLOF. Upper panel represents the whole hydrogen profile while the lower one highlights the bottom of the profile. The evolution of the outer parts of the profile are fully dominated by diffusion. In the bottom there is an interplay between nuclear burning and diffusion. Initially nuclear reactions dominate (models 14500 to 15050), but at later times (model 15075) chemical diffusion drives a large amount of hydrogen inwards.

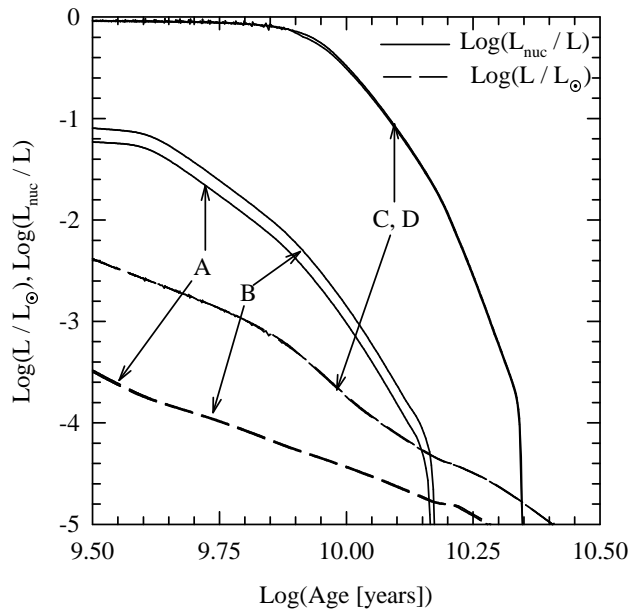


**Figure 9.** The logarithm of photon luminosity and nuclear luminosity fraction released during the last stages of evolution of the models considered in this paper. Labels A, B, C, D refer to the evolutionary tracks A to D in Fig. 1. Models without diffusion have a much larger nuclear activity at advanced evolutionary stages, which slows down the evolution in an appreciable way. Remarkably, the ages of these objects are largely determined by the allowance of diffusion whereas considering or neglecting thermonuclearly induced RLOFs has a negligible effect on stellar ages.